Published in final edited form as:
Astrophys J Lett. ; 851: . doi:10.3847/2041-8213/aaa01b.

First Detection of Interstellar S_2H

Asunción Fuente[1], **Javier R. Goicoechea**[2], **Jerome Pety**[3,4], **Romane Le Gal**[5], **Rafael Martín-Doménech**[5], **Pierre Gratier**[6], **Viviana Guzmán**[7], **Evelyne Roueff**[8], **Jean Christophe Loison**[9], **Guillermo M. Muñoz Caro**[10], **Valentine Wakelam**[6], **Maryvonne Gerin**[4], **Pablo Riviere-Marichalar**[2], and **Thomas Vidal**[6]

[1]Observatorio Astronómico Nacional (OAN,IGN), Apdo 112, E-28803 Alcalá de Henares, Spain

[2]Instituto de Ciencia de Materiales de Madrid (ICMM-CSIC), Sor Juana Ins de la Cruz, 3, E-28049 Cantoblanco, Madrid, Spain

[3]Institut de Radioastronomie Millimétrique (IRAM), 300 rue de la Piscine, 38406 Saint Martin d'Hères, France

[4]LERMA, Observatoire de Paris, PSL Research University, CNRS, Sorbonne Universités, UPMC Univ. Paris 06, Ecole Normale Supérieure, F-75005 Paris, France

[5]Harvard-Smithsonian Center for Astrophysics, 60 Garden St., Cambridge, MA 02138, USA

[6]Laboratoire d'Astrophysique de Bordeaux, Univ. Bordeaux, CNRS, B18N, allée Geoffroy Saint-Hilaire, 33615 Pessac, France

[7]Joint ALMA Observatory (JAO), Alonso de Córdova 3107, Vitacura, Santiago, Chile

[8]LERMA, Observatoire de Paris, PSL Research University, CNRS, Sorbonne Universités, UPMC Univ. Paris 06, F-92190 Meudon, France

[9]Institut des Sciences Moléculaires de Bordeaux (ISM), CNRS, Univ. Bordeaux, 351 cours de la Libération, 33400, Talence, France

[10]Centro de Astrobiología (CSIC-INTA), Carretera de Ajalvir, km 4, Torrejón de Ardoz, 28850 Madrid, Spain

Abstract

We present the first detection of gas phase S_2H in the Horsehead, a moderately UV-irradiated nebula. This confirms the presence of doubly sulfuretted species in the interstellar medium and opens a new challenge for sulfur chemistry. The observed S_2H abundance is $\sim 5\times10^{-11}$, only a factor 4-6 lower than that of the widespread H_2S molecule. H_2S and S_2H are efficiently formed on the UV-irradiated icy grain mantles. We performed ice irradiation experiments to determine the H_2S and S_2H photodesorption yields. The obtained values are $\sim 1.2\times10^{-3}$ and $<1\times10^{-5}$ molecules per incident photon for H_2S and S_2H, respectively. Our upper limit to the S_2H photodesorption yield suggests that photo-desorption is not a competitive mechanism to release the S_2H molecules to the gas phase. Other desorption mechanisms such as chemical desorption, cosmic-ray desorption and grain shattering can increase the gaseous S_2H abundance to some extent.

Corresponding author: Asunción Fuente, a.fuente@oan.es.

Europe PMC Funders Author Manuscripts

Alternatively, S_2H can be formed via gas phase reactions involving gaseous H_2S and the abundant ions S^+ and SH^+. The detection of S_2H in this nebula could be therefore the result of the coexistence of an active grain surface chemistry and gaseous photo-chemistry.

Keywords

Astrochemistry; methods: laboratory: solid state; ISM: abundances; ISM: molecules; photon-dominated region (PDR); Horsehead

1 Introduction

Sulfur is one of the most abundant elements in the Universe (S/H~1.3×10^{-5}) and plays a crucial role in biological systems on Earth, so it is important to follow its chemical history in space. Surprisingly, sulfuretted molecules are not as abundant as expected in the interstellar medium. A few sulfur compounds have been detected in diffuse clouds demonstrating that the sulfur abundance in these low density regions is close to the cosmic value (Neufeld et al. 2015). A moderate sulfur depletion (a factor of 4) is observed in the external layers of the photodissociation region (PDR) in the Horsehead nebula, as well (Goicoechea et al. 2006). In cold molecular clouds, a large depletion of sulphur is usually considered to reproduce the observations (see for instance Tieftrunk et al. 1994). However, recent models by Vidal et al. (2017) explained the observational data without or with little sulfur depletion after updating the gas and grain chemistry. In that case, HS and H_2S on the grains or atomic sulphur in the gas would contain most of the sulfur. In hot cores and corinos, Wakelam et al. (2004) found that observations of S-bearing molecules would be better reproduced if sulfur was sublimated from grains in the atomic form or it is quickly converted into it. Thus far, the main solid or gas sulfur carrier is still debated.

With an adsorption energy of ~1100 K (Hasegawa & Herbst 1993), sulfur atoms are expected to stick on the surfaces of grains with temperatures below ~22 K. Here, because of the high hydrogen abundances and the mobility of hydrogen in the ice matrix, sulfur atoms are expected to form H_2S. Indeed, gaseous H_2S is the most abundant S-bearing molecule in comets, with an abundance of up to 1.5% relative to water (Bockelée-Morvan et al. 2000). A firm detection of H_2S in interstellar ices has not been reported yet. A realistic upper limit of the H_2S abundance in interestellar ices is 1% relative to water that is 10 times lower than the cosmic abundance (Jiménez-Escobar & Muñoz Caro 2011). One possibility to explain the low fraction of H_2S in interstellar ices is that H_2S is processed by UV-photons or cosmic rays in the ice leading to the formation of other S-bearing species. OCS and tentatively SO_2 have been detected in icy mantles but their abundances are far too low to explain the missing S budget (Geballe et al. 1985; Palumbo et al. 1995; Boogert et al. 1997).

Trying to provide new insights into the ice composition, experimental simulations of the irradiation of interstellar ices containing H_2S under astrophysically relevant conditions have been performed in laboratoty using UV photons (Jiménez-Escobar & Muñoz Caro 2011; Jiménez-Escobar et al. 2014), X-rays (Jiménez-Escobar et al. 2012), or ions (Moore et al. 2007; Ferrante et al. 2008; Garozzo et al. 2010). Energetic processing of H_2S-bearing ices readily generates sulfur-sulfur bonds, and the main S-bearing products in these experiments

Europe PMC Funders Author Manuscripts

are H_2S_2 and S_2H that were detected by Jiménez-Escobar & Muñoz Caro (2011) through their infrared absorption bands. The molecule H_2S_2 could subsequently photodissociate forming S_2 and S_3 depending on the irradiation time. These molecules with two S atoms and even more could thus contain a significant fraction of the missing sulfur in dense clouds. In line with this work, Druard & Wakelam (2012) suggested that polysulphanes could be a sulfur reservoir in the ice and are rapidly converted into atomic sulfur once in the gas phase. Martín-Doménech et al. (2016a) unsuccesfully searched for S_2H and H_2S_2 in the gas phase toward the well-known hot corino, IRAS 16293−2422. The lack of gaseous S_2H and H_2S_2 was interpreted as the consequence of the rapid destruction of these species once sublimated in such a warm and dense environment (Martín-Doménech et al. 2016a; Fortenberry & Francisco 2017).

In this Letter, we report the first interstellar detection of S_2H in the prototypical photo-dissociation region, the Horsehead. In Sect. 4, we discuss the possible grain-surface and gas-phase S_2H formation routes. New measurements of the photodesorption yields of S_2H and H_2S are presented in Sect. 5.

2 Observations and Data Reduction

The data used in this work are from the Horsehead WHISPER (Wide-band High-resolution Iram-30m Surveys at two Positions with Emir Receivers, PI: J. Pety) project and the Director's Discrectionary Time project D11-16. The Horsehead WHISPER project is a complete unbiased line survey of the 3, 2, and 1 mm bands using the IRAM 30m telescope. Two positions are observed: i) the HCO peak (RA=$5^h40^m53^s.936$, Dec=2°28′00″, J2000), which is characteristic of the photo-dissociation region at the UV-illuminated surface of the Horsehead nebula (Gerin et al. 2009) (also referred to as PDR position), and ii) the DCO^+ peak (RA=$5^h40^m55^s.61$, Dec=2°27′38″, J2000), which corresponds to a cold and UV-shielded condensation located less than 40″ away from the PDR edge (Pety et al. 2007). During the observations we used the Position-Switching procedure with the reference position located at an offset (−100″,0) relative to RA: $05^h40^m54^s.27$ Dec: −02°28′00″.0. Several lines of S_2H were tentatively detected towards the two positions observed in the WHISPER survey. In order to confirm the S_2H detection, we requested Director's Discrectionay Time (D11-16) to observe a single setup covering the frequencies listed in Table 1. The merged S_2H spectra are shown in Fig. 1. Line intensities are given in main brightness temperature (T_{MB}) and the lines were observed with a frequency resolution of 49 kHz.

In order to have a deeper insight into the S_2H chemistry, we compare the new S_2H observations with the H_2S $1_{1,0}\rightarrow1_{0,1}$ map observed during April 2006 with the IRAM 30m telescope. These observations were done using the frequency switching mode and a spectral resolution of 40 kHz. Averaged noise level per resolution element at 168 GHz is rms(T_{MB})=170 mK. The integrated intensity emission of the H_2S line varies between $1.0^{-1.5}$ K km s^{-1} across the molecular cloud with an abrupt border in the west (see Fig. 1). The H_2S emission presents a local minimum towards the DCO^+ peak, similar to the morphology observed in other species such as CH_3OH (Guzmán et al. 2011, 2013), suggesting gaseous H_2S depletion towards this cold dense core.

3 Column Densities and Abundances

The rotational spectrum of S_2H was calculated by Tanimoto et al. (2000). The spectroscopic data can be found in the CDMS catalogue (Müller et al. 2005). We have detected eight S_2H lines located at 94526.1508, 94526.3208, 94731.0115, 94731.2080, 110294.0282, 110294.1530, 110497.9666, and 110498.1104 MHz. The S_2H hyperfine transitions are forming doublets very close in frequency (~0.12 MHz) that remain unresolved in our data (see Fig. 1). In Table 1, we show the Gaussian fits to the observed line features, each one clearly detected with S/N>5. We have adopted as central frequency the one of the most intense component of the doublet. For this reason the central velocity shown in Table 1 is systematically shifted by ~0.2−0.5 km s^{-1} from the Horsehead systemic velocity, 10.5 km s^{-1}. We have checked possible contamination by other compounds using the CDMS and JPL catalogues. There is no other good candidate to be a carrier of these lines. The large linewidth of the 94.731 GHz line towards the DCO^+ peak position, ~1.7 km s^{-1}, is more likely due to the poor baseline around this feature.

The WEEDS software has been used to simulate the S_2H spectrum in the whole frequency coverage of the WHISPER survey assuming LTE conditions. We have fitted the detections and upper-limits of 97 lines with upper level energies lower than 75 K found in the frequency range of the full survey using the Bayesian method described by Majumdar et al. (2017). The whole spectrum can be fitted assuming that the emission uniformly fills the beam and the rotation temperatures and S_2H column densities listed in Table 1. The fitted line-widths are 0.68±0.12 km s^{-1} for the core and 0.63±0.1 km s^{-1} for the PDR. The observed S_2H linewidths are consistent with the emission coming from the UV irradiated gas. Species that are more abundant in the cold and UV shielded gas of the core as DCO^+ and $H^{13}CO^+$, present narrower line-widths towards the DCO^+ peak than towards the PDR (Goicoechea et al. 2009). However, others PDR-like species such as HCO present similar linewidths towards both positions (Gerin et al. 2009). This suggests that even towards the core position, the S_2H emission is mainly coming from the UV-illuminated layers of the cloud along the line of sight.

The S_2H rotation temperatures reveal subthermal excitation and are similar to those derived for other high dipole moment compounds like o-H_2CO (Guzmán et al. 2011). The estimated abundance (wrt hydrogen nuclei) is ~5×10^{-11} towards the DCO^+ peak and about a factor of 2 larger towards the HCO peak.

From the chemical point of view, it is interesting to compare the S_2H abundance with those of the related species H_2S. Unfortunately there is only one transition of H_2S that is easily observable with the 30m telescope given the physical conditions in the Horsehead, the o-H_2S $1_{1,0}\rightarrow1_{0,1}$ line. Thus, we need to assume a rotation temperature to derive the H_2S column density. Since the H_2S dipole moment (μ_b=0.978 D; Viswanathan et al. 1984) is similar to those of S_2H (μ_a=1.161 D, μ_b=0.827 D; Peterson et al. 2008), we assume the same rotation temperature for both molecules. With these assumptions and adopting an ortho-to-para ratio of 3, we derive a H_2S abundance of ~3×10^{-10} towards the two positions. This would imply that $[S_2H]/[H_2S]$=0.15±0.09 in the DCO^+ peak and $[S_2H]/[H_2S]$=0.27±0.14, toward the HCO peak. These numbers are consistent with the $[S_2H]/[H_2S]$ ice ratio obtained

by Jiménez-Escobar et al. (2012) in their simulations of UV irradiation of H_2S ices. In the following, we qualitatively explore the possible surface and gas-phase formation routes of S_2H.

4 S_2H Formation

The formation of S_2H is a intricate problem due to the low H-SS energy bonding. Evidences for the formation of S_2H during irradiation of pure H_2S and H_2S:H_2O ice mixtures were provided by Jiménez-Escobar & Muñoz Caro (2011) using the same experimental setup as the one described here. One way of forming S_2H could be the grain surface reactions: s-H atom (hereafter, 's-' is used to refer to the solid phase) addition on s-S_2, and s-S + s-HS reaction, followed by chemical desorption. However, the low exothermicity of the first reaction should prevent efficient chemical desorption (Minissale et al. 2016; Wakelam et al. 2017). The second reaction should not be efficient in cold cores because, below 15 K, S atom and HS radical are not mobile on ice considering the adsorption energies given by Wakelam et al. (2017). Moreover, S_2H is a very reactive species in the gas phase, reacting with H, N, C and O atoms without barrier, so likely also on surface. An alternative surface induced S_2H production may be s-H_2S_2 photo-dissociation-desorption: s-H_2S_2 + hν→S_2H +H. s-H_2S_2 may be efficiently produced by the s-HS + s-HS reaction but it needs mobile HS on ice and so a high grain temperature.

In the gas-phase, S_2H may be produced by the electronic dissociative recombination of $H_2S_2^+$. Even if there is no data on this reaction, the loss of one H atom is always an important exit channel on dissociative recombination (Plessis et al. 2010). There are two known $H_2S_2^+$ production pathways: the $S^+ + H_2S \rightarrow H_2S_2^+ + h\nu$ reaction (Anicich, V.G. 2003), despite the fact that the reference is an unpublished work and previous experimental studies did not identify this channel (Smith et al. 2004), and the $SH^+ + H_2S \rightarrow H_2S_2^+ + H$ reaction which is well characterized (Anicich, V.G. 2003). We note that S^+ and SH^+ are only abundant in the UV-irradiated gas (Gerin et al. 2016). Therefore, in spite of the large uncertainties in the reaction rates, we can conclude that these formation routes are only efficient in the UV-illuminated cloud surfaces.

5 Experimental Study of the Photodesorption of S_2H and H_2S

Jiménez-Escobar & Muñoz Caro (2011) showed that sulfur-sulfur bonds, in particular H_2S_2 and S_2H, are formed in irradiated ices. Here we focus on the determination of the S_2H and H_2S photodesorption yields which are key to determine the origin (surface vs gas phase chemistry) of the observed S_2H. For this aim, we performed experimental simulations under astrophysically relevant conditions using the ISAC setup (Muñoz Caro et al. 2010), an ultra-high vacuum chamber with a work pressure on the order of 4×10^{-11} mbar, corresponding to the pressure found in the interior of the pre-stellar cores. Sulfur is expected to be locked on the icy mantles in these regions, H_2S being the most abundant S-bearing molecule in cometary ices. Pure amorphous H_2S ice samples with thicknesses of about 40×10^{15} molecules cm^{-2} were deposited from the gas phase (H_2S gas, Praxair, 99.8%) onto a KBr

substrate at 8 K, and subsequently irradiated using an F-type microwave-discharged hydrogen flow lamp with a vaccum-ultraviolet flux of 2×10^{14} photons cm^2 s^{-1} at the sample position (Muñoz Caro et al. 2010). The emission spectrum of the lamp (reported in Chen et al. 2014, and Cruz-Diaz et al. 2014) resembles that of the secondary UV field in dense cloud interiors, calculated by Gredel et al. (1989). A Pfeiffer Prisma quadrupole mass spectrometer (QMS) was used during irradiation of the ice samples to monitor the mass fragments m/z = 34 (corresponding to photodesorbing H_2S molecules), and m/z = 64 (corresponding to any desorbing photoproduct with a sulfur-sulfur bond, observed to form in Jiménez-Escobar et al. (2012)). In our experiment, we did not monitore S_2H directly. However, if H_2S_2 or S_2H were desorbed, we would expect to detect all the fragments derived from these species, in particular S_2^+. While photodesorption of H_2S was detected, no gaseous S_2^+ was observed (see Fig. 2). The measured ion current was converted into a photodesorption yield following calibration of the QMS (see Martín-Doménech et al. 2015). Photodesorption of H_2S took place with a decreasing yield, reaching a steady-state value of 1.2×10^{-3} molecules per incident photon after ~30 minutes of irradiation, which corresponds to the fluence experienced by ice mantles during the typical cloud lifetime (Shen et al. 2004). A factor of 2 is assumed as the error in the photodesorption yield values due to the uncertainties in the calibration process, see Martín-Doménech et al. 2016b. Following the non-detection of any sulfur-sulfur photo-product, an upper limit of 1×10^{-5} molecules per incident photon (the sensitivity limit of our QMS) was assumed for the photodesorption of S_2H. Direct S_2H photodesorption or H_2S_2 photo-dissociation-desorption are therefore not expected to be the origin of the gaseous S_2H.

6 Discussion and Conclusions

At a distance of 400 pc, the Horsehead is a PDR viewed nearly edge-on and illuminated by the O9.5V star σOri at a projected distance of ~3.5 pc. The intensity of the incident FUV radiation field is χ=60 relative to the interstellar radiation field in Draine units. This PDR presents a differentiated chemistry from others associated with nearby HII regions such as the Orion Bar. One main difference is that the dust temperature is around ~20-30 K in the PDR (Goicoechea et al. 2009), i.e. below or close to the sublimation temperature of many species, allowing a rich surface chemistry on the irradiated surfaces. Our unbiased line survey has provided valuable hints on the chemistry of this region. The detection of the molecular ions CF^+ and HOC^+ towards the HCO peak are well understood in terms of gas-phase photochemistry (Guzmán et al. 2012). We learned that there is an efficient top-down chemistry in the PDR, in which large polyatomic molecules or small grains are photo-destroyed into smaller hydrocarbon molecules/precursors, such as C_2H, C_3H_2, C_3H and C_3H^+ (Pety et al. 2012; Guzmán et al. 2015). The detection of several complex organic molecules (COMs) towards the warm (T_{kin} ~ 60 K) PDR and its associated cold (T_{kin} ~ 20 K) core was unexpected. In fact, the chemical complexity reached in the Horsehead is extraordinarily high with COMs of up to 7 atoms: HCOOH, H_2CCO, CH_3CHO and CH_3CCH (Guzmán et al. 2014). Current pure gas-phase models cannot reproduce the inferred H_2CO, CH_3OH and COMs abundances in the Horse-head PDR (Guzmán et al. 2011, 2013), which supports the grain surface origin of these molecules. Le Gal et al. (2017) was able to reproduce the observed COMs abundances using a chemical model with grain

surface chemistry and found that chemical desorption, instead of photodesorption, is the main process to release COMs to the gas phase. CH_3CN and CH_3NC, key species for the formation of prebiotic molecules, seem to have a very specific formation pathway in the PDR (Gratier et al. 2013). The Horsehead is therefore an excellent site to study the influence of UV radiation on the grain surface chemistry and its subsequent impact on the gas phase.

We present the first detection of S_2H in the Horse-head. The observed S_2H abundance is $\sim 5\times10^{-11}$, only a factor 4-6 lower than that of H_2S. Our laboratory experiments show that the H_2S and S_2H photodesortion yields are 1.2×10^{-3} and $<1\times10^{-5}$ molecules per incident photon, respectively. Although S_2H can be formed on warm (T_d>15 K) grains, our upper limit to the S_2H photodesorption yield suggest that this mechamism is not efficient to release the S_2H molecules from the grain mantles. Other desorption mechanisms such as chemical desorption, cosmic-ray desorption and grain shattering could increase the S_2H abundance in gas phase. S_2H can also be formed in gas-phase by reactions involving H_2S and the ions S^+ and SH^+. These ions are expected to be abundant in the external layers of the PDR (Goicoechea et al. 2006). The photodesorption of H_2S could hence boost the S_2H production in gas phase. We conclude that the abundance of S_2H in the Horsehead is more likely the consequence of the favorable physical conditions prevailing in this nebula where grain mantles irradiated by UV photons coexist with the ions S^+ and SH^+ that are only abundant in PDRs.

One interesting issue is to compare the sulfur and oxygen chemistry. We have not detected H_2S_2, HSO, H_2O_2 and HO_2 in the Horsehead with the upper limits shown in Table 3. We find interesting that the column densities of HSO and HO_2 are lower than that of S_2H, although the oxygen elemental abundance is 30 times greater than that of sulfur. In gas phase, S_2H is mainly formed through $S^+ + H_2S \rightarrow H_2S_2^+ + h\nu$ and $SH^+ + H_2S \rightarrow H_2S_2^+ + H$ followed by dissociative recombination of $H_2S_2^+$. Oxygen and sulfur have indeed similar reactivity but, due to their different ionization potentials, O^+ is expected less abundant than S^+ and then the O^+ and OH^+ reactions play a smaller role. We have also compared the $SH^+ + H_2O$ and $SH^+ + H_2S$ gas-phase reactions which may be intermediate paths at work for producing SOH and S_2H, respectively. The channel towards $HSO^+ + H_2$ reaction is endothermic in opposite to the channels towards $S_2H^+ + H_2$ and $S_2H_2^+ + H$. Therefore, in gas phase the formation of S_2H is favored relative to HSO. HSO and related species have not been observed in space thus far (Cazzoli et al. 2016; Fortenberry & Francisco 2017). Laboratory experiments demonstrate that grain surface chemistry involving H_2O and H_2S also present different pathways. Photo-desorption experiments reported by Cruz-Diaz et al. (2017) show that H_2O_2 is not formed in UV irradiated water ice. In contrast, Jiménez-Escobar & Muñoz Caro (2011) showed that H_2S_2 is formed when a H_2S and H_2S-H_2O ices are irradiated, providing a path to form species with two sulfur atoms. Summarizing, sulfur and oxygen are not analogues in the gas-phase and surface chemistry, and the comparison of their related species requires the full chemical modelling of the region.

Europe PMC Funders Author Manuscripts

Acknowledgments

We thank the Spanish MINECO for funding support from AYA2016-75066-C2-1/2-P, AYA2012-32032 and ERC under ERC-2013-SyG, G. A. 610256 NANOCOSMOS. This work was supported by the Programme National "Physique et Chimie du Milieu Interstellaire" (PCMI) of CNRS/INSU with INC/INP co-funded by CEA and CNES.

References

Anicich, VG. JPL Publication 2003, 03-19 NASA; 2003.

Bockelée-Morvan D, Lis DC, Wink JE, et al. A&A. 2000; 353:1101.

Boogert ACA, Schutte WA, Helmich FP, Tielens AGGM, Wooden DH. A&A. 1997; 317:929.

Cazzoli G, Lattanzi V, Kirsch T, et al. A&A. 2016; 591:A126.

Chen Y-J, Chuang K-J, Muñoz Caro GM, et al. ApJ. 2014; 781:15.

Cruz-Diaz GA, Muñoz Caro GM, Chen Y-J, Yih T-S. A&A. 2014; 562:A119.

Cruz-Diaz GA, Martín-Doménech R, Moreno E, Muñoz Caro GM, Chen Y-J. arXiv:1711.05679. 2017

Druard C, Wakelam V. MNRAS. 2012; 426:354.

Ferrante RF, Moore MH, Spiliotis MM, Hudson RL. ApJ. 2008; 684:1210.

Fortenberry RC, Francisco JS. ApJ. 2017; 835:243.

Garozzo M, Fulvio D, Kanuchova Z, Palumbo ME, Strazzulla G. A&A. 2010; 509:A67.

Geballe TR, Baas F, Greenberg JM, Schutte W. A&A. 1985; 146:L6.

Gerin M, Goicoechea JR, Pety J, Hily-Blant P. A&A. 2009; 494:977.

Gerin M, Neufeld DA, Goicoechea JR. ARA&A. 2016; 54:181.

Goicoechea JR, Pety J, Gerin M, et al. A&A. 2006; 456:565.

Goicoechea JR, Compiègne M, Habart E. ApJl. 2009; 699:L165.

Gredel R, Lepp S, Dalgarno A, Herbst E. ApJ. 1989; 347:289.

Gratier P, Pety J, Guzmán V, et al. A&A. 2013; 557:A101.

Guzmán V, Pety J, Goicoechea JR, Gerin M, Roueff E. A&A. 2011; 534:A49.

Guzmán V, Pety J, Gratier P, et al. A&A. 2012; 543:L1.

Guzmán VV, Goicoechea JR, Pety J, et al. A&A. 2013; 560:A73.

Guzmán VV, Pety J, Gratier P, et al. Faraday Discussions. 2014; 168:103. [PubMed: 25302376]

Guzmán VV, Pety J, Goicoechea JR, et al. ApJl. 2015; 800:L33.

Hasegawa TI, Herbst E. MNRAS. 1993; 261:83.

Jiménez-Escobar A, Muñoz Caro GM. A&A. 2011; 536:A91.

Jiménez-Escobar A, Muñoz Caro GM, Cicarelli A, Cecchi-Pestellini C, Candia R, Micela G. ApJL. 2012; 751:L40.

Jiménez-Escobar A, Muñoz Caro GM, Chen Y-J. MNRAS. 2014; 443:343.

Le Gal R, Herbst E, Dufour G, et al. A&A. 2017; 605:A88.

Majumdar L, Gratier P, Andron I, Wakelam V, Caux E. MNRAS. 2017; 467:3525.

Martín-Doménech R, Manzano-Santamaría J, Muñoz Caro GM, et al. A&A. 2015; 584:A14.

Martín-Doménech R, Jiménez-Serra I, Muñoz Caro GM, et al. A&A. 2016; 585:A112.

Martín-Doménech R, Muñoz Caro GM, Cruz-Díaz GA. A&A. 2016; 589:A107.

Minissale M, Dulieu F, Cazaux S, Hocuk S. A&A. 2016; 585:A24.

Moore MH, Hudson RL, Carlson RW. Icarus. 2007; 189:409.

Müller HSP, Schlöder F, Stutzki J, Winnewisser G. J Mol Struct. 2005; 742:215.

Muñoz Caro GM, Jiménez-Escobar A, Martín-Gago JÁ, et al. A&A. 2010; 522:A108.

Neufeld DA, Godard B, Gerin M, et al. A&A. 2015; 577:A49.

Palumbo ME, Tielens AGGM, Tokunaga AT. ApJ. 1995; 449:674.

Plessis S, Carrasco N, Pernot P. J Chem Phys. 2010; 133:13.

Peterson KA, Mitrushchenkov A, Francisco JS. Chem Phys. 2008; 346:34.

Pety J, Goicoechea JR, Hily-Blant P, Gerin M, Teyssier D. A&A. 2007; 464:L41.
Pety J, Gratier P, Guzmán V, et al. A&A. 2012; 548:A68.
Shen CJ, Greenberg JM, Schutte WA, van Dishoeck EF. A&A. 2004; 415:203.
Smith D, Adams NG, Lindinger W. The Journal of Chemical Physics. 1981; 75(7):3365.
Tanimoto M, Klaus T, Müller HSP, Winnewisser G. J Mol Spectrosc. 2000; 199:73. [PubMed: 10712872]
Tieftrunk A, Pineau des Forets G, Schilke P, Walmsley CM. A&A. 1994; 289:579.
Vidal THG, Loison J-C, Jaziri AY, et al. MNRAS. 2017; 469:435.
Viswanathan R, Dyke TR. J Mol Spectrosc. 1984; 103:231.
Wakelam V, Caselli P, Ceccarelli C, Herbst E, Castets A. A&A. 2004; 422:159.
Wakelam V, Loison J-C, Mereau R, Ruaud M. Molecular Astrophysics. 2017; 6:22.

Europe PMC Funders Author Manuscripts

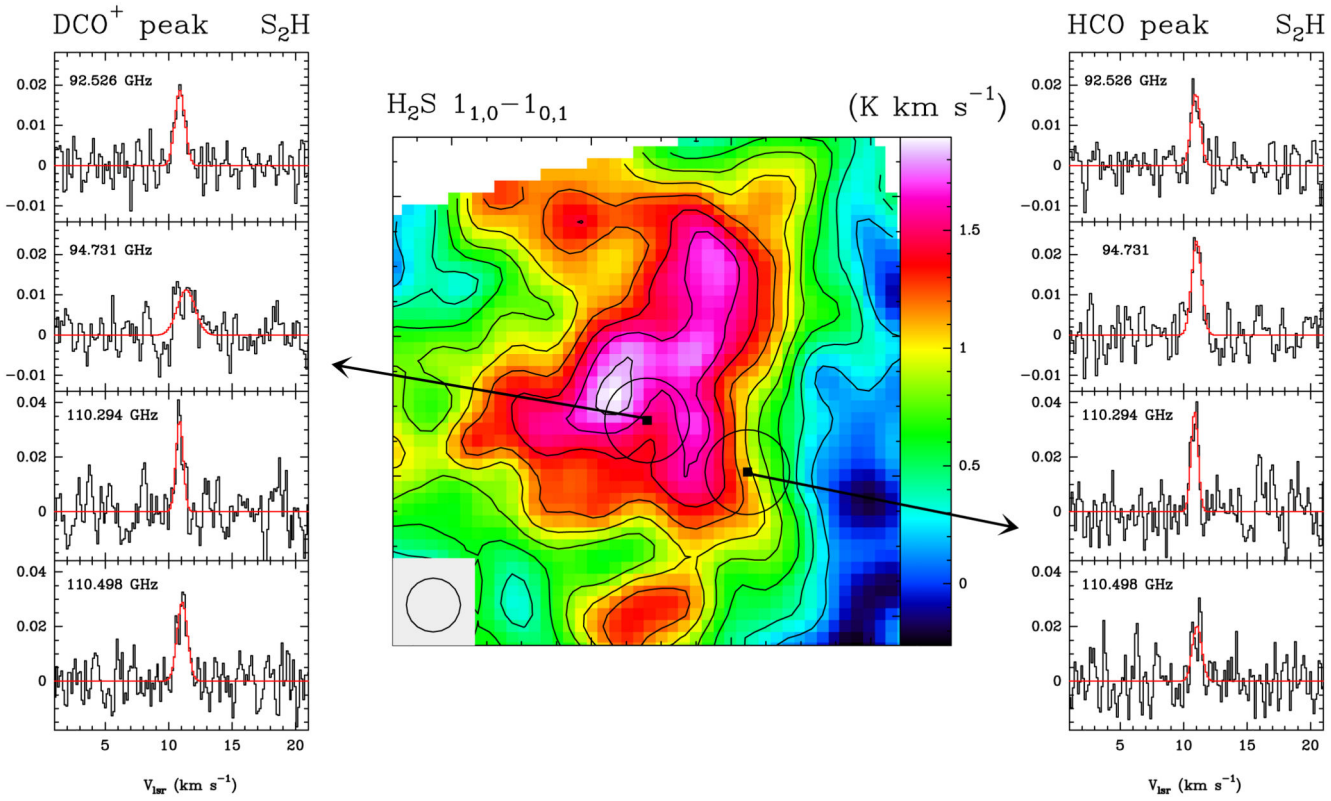

Figure 1.

In the central panel, we show the integrated intensity map of the H_2S $1_{1,0}\rightarrow1_{0,1}$ line (168.763 GHz). UV-illumination from σOri comes from the west (right). The beam is drawn in the bottom-left corner. Black circles around the surveyed positions indicate the beam of the S_2H detections. Spectra of the four S_2H lines detected towards the two positions targetted in the Whisper spectral are plotted in the left (DCO^+ peak) and right (HCO peak) panels. The frequency in GHz is indicated in the top-left corner. In red, the Gaussian fits shown in Table 1.

Europe PMC Funders Author Manuscripts

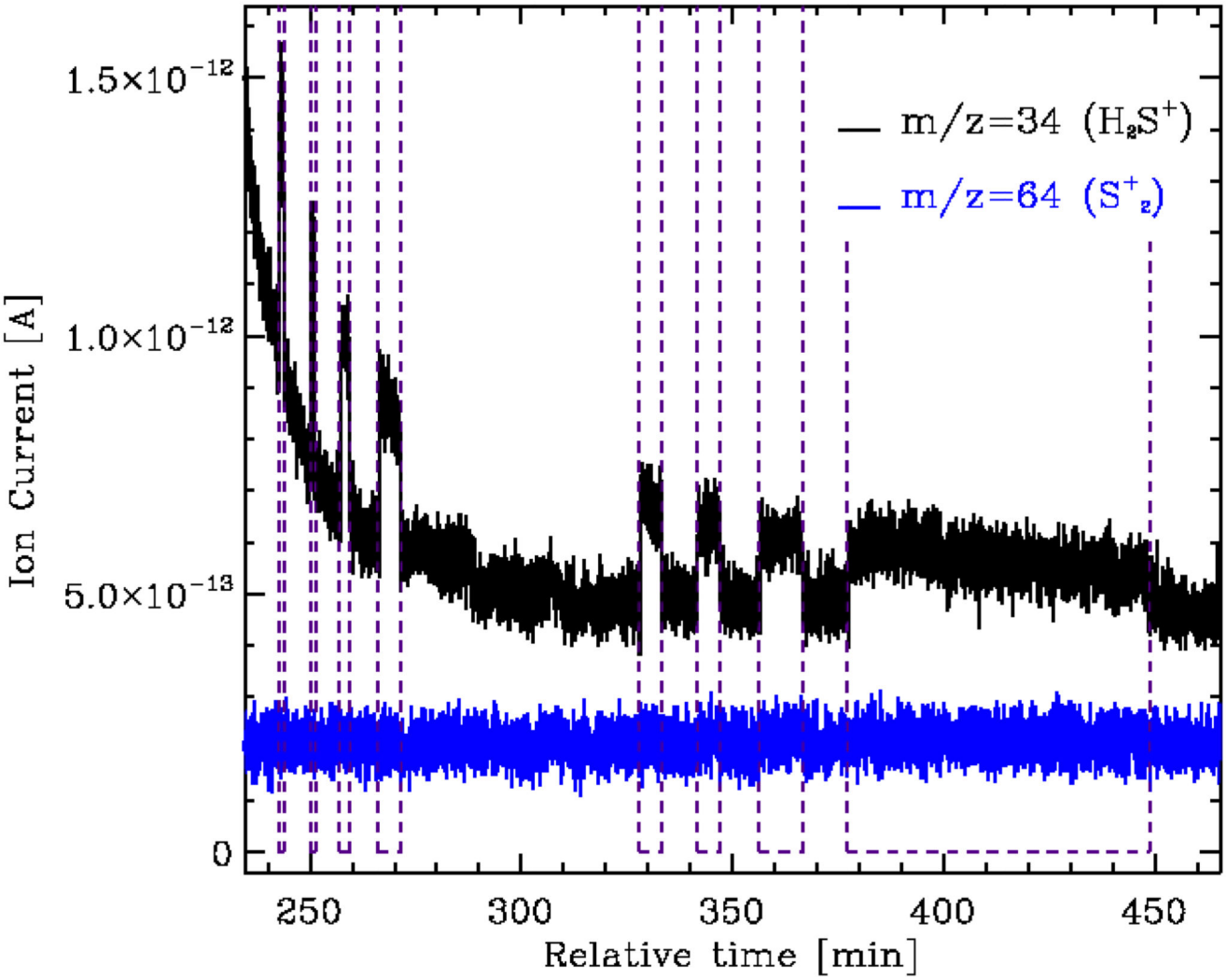

Figure 2.

Photodesorption of H_2S (black) detected by the QMS during irradiation of a pure H_2S ice sample. No increase of the measured ion current for the mass fragment $m/z = 64$ (blue, corresponding to any sulfur-sulfur photo-product) was detected. Irradiation intervals are indicated with vertical dashed lines. Signals are shifted for clarity.

Europe PMC Funders Author Manuscripts

Table 1

Gaussian fits

Freq(MHz)	Area(K kms^{-1})	v_{lsr}(km s^{-1})	Δv(km s^{-1})	T_{MB}(K)	rms (K)
DCO^+ peak (core)					
94526.32	0.019 (0.002)	10.90 (0.05)	0.9 (0.1)	0.018	0.004
94731.21	0.020 (0.003)	11.39 (0.13)	1.7 (0.2)	0.011	0.004
110294.15	0.024 (0.004)	10.86 (0.05)	0.7 (0.1)	0.033	0.008
110498.11	0.029 (0.004)	11.09 (0.06)	0.9 (0.1)	0.029	0.007
HCO peak (PDR)					
94526.32	0.016 (0.002)	10.97 (0.06)	0.9 (0.1)	0.018	0.004
94731.21	0.023 (0.003)	11.03 (0.05)	0.9 (0.1)	0.023	0.004
110294.15	0.026 (0.003)	10.87 (0.04)	0.7 (0.1)	0.037	0.008
110498.11	0.019 (0.004)	11.07 (0.09)	0.9 (0.2)	0.020	0.007

Table 2

Summay of column densities and fractional abundances

Molecule			DCO^+ peak			HCO peak	
	HPBW (″)	T_{rot} (K)	N(X) (cm^{-2})	$N(X)/N_H$	T_{rot} (K)	N(X) (cm^{-2})	$N(X)/N_H$
H_2	12		2.9×10^{22}	0.5		1.9×10^{22}	0.5
S_2H	22 - 26	$8.73^{+1.36}_{-1.10}$	$3.0^{+0.9}_{-0.6}\times10^{12}$	$5.2^{+1.5}_{-1.0}\times10^{-11}$	$12.69^{+1.78}_{-1.54}$	$3.3^{+1.2}_{-0.7}\times10^{12}$	$8.7^{+3.1}_{-1.9}\times10^{-11}$
H_2S [1]	14	9^{+1}_{-1}	$1.9^{+0.4}_{-0.3}\times10^{13}$	$3.3^{+0.7}_{-0.6}\times10^{-10}$	12^{+2}_{-2}	$1.2^{+0.1}_{-0.2}\times10^{13}$	$3.1^{+0.3}_{-0.5}\times10^{-10}$

(1) We assume the rotation temperatures derived from S_2H.

Europe PMC Funders Author Manuscripts

Table 3

Column density upper limits

Molecule	Freq (GHz)	rms[1] (mK)	N_X[2] (cm^{-2})
S_2H_2	139.885	9	$<8.5\times10^{11}$
HSO	158.391	30	$<1.5\times10^{12}$
HO_2	130.260	11	$<4.7\times10^{11}$
H_2O_2	90.365	4	$<1.0\times10^{12}$

(1) The rms has been calculated for a channel width of ≈0.3 km s^{-1}. The obtained rms is similar in the two surveyed positions.

(2) 3σ upper limits assuming LTE, T_{rot}=10 K and a linewidth of 0.6 km s^{-1}